

## Surgical Wound Healing Using Polyurethane Dressings Incorporated with Walnut Leaf Extract

Poodineh Hajipoor F. PhD<sup>1\*</sup>, Hosseini H. PhD<sup>2</sup>

### Abstract:

**Background and Objective:** Skin loss may occur due to various causes, including genetic disorders, acute trauma, chronic wounds, or even surgical interventions. Dressings can accelerate wound healing by protecting the wound from bacterial contamination and providing a favorable environment for tissue repair. Moist wound dressings are particularly effective in preventing dressing-related injuries, managing exudates, and minimizing discomfort and pain. In this study, a polyurethane-based film incorporated with walnut leaf extract was developed and evaluated.

**Materials & Methods:** To prepare the polyurethane biofilm, a 12% polyurethane solution was formulated using tetrahydrofuran and dimethylformamide (50:50). Walnut leaf extract was then added at concentrations of 1%, 2%, and 4% (w/w), followed by casting into Teflon molds. Physicochemical and mechanical properties were assessed using Fourier-transform infrared spectroscopy (FTIR), light transmittance, swelling behavior in phosphate-buffered saline (PBS), degradation analysis, and cytotoxicity testing. The tensile strength of the films decreased with increasing extract content, while flexibility improved.

**Results:** Due to the diverse chemical constituents of the extract, elongation at break increased from  $38.4 \pm 4.7\%$  to  $68.24 \pm 11.3\%$ . Swelling capacity in PBS rose from 76% for pure polyurethane to 96% for films containing 4% extract. MTT assay results indicated no cytotoxicity for films containing 1% and 2% extract, whereas the 4% extract film exhibited cytotoxic effects.

**Conclusion:** Based on the analytical data and SEM observations of L929 fibroblast cells cultured on the films, it can be concluded that polyurethane films containing 2% walnut leaf extract provide optimal mechanical, chemical, physical, and biological properties, making them suitable candidates for skin tissue applications in surgical wound healing.

**Keywords:** Polyurethane, Walnut leaf extract, Biofilm, Wound dressing

<sup>1</sup> Ph.D. in Biomedical Engineering, Zahedan University of Medical Sciences, Zahedan, Iran

<sup>2</sup> Ph.D. in Microbiology, Zahedan University of Medical Sciences, Zahedan, Iran

Received: 15/09/2025

Accepted: 04/04/2026

**Corresponding Author: Dr. Fatemeh Poodineh Hajipoor**

Tel: 05433222508

E-mail: fatemehpoodinehhajipoor@gmail.com

## Background and Objective

The skin is the largest organ of the human body and serves as a protective barrier between the body and the external environment, shielding underlying tissues from microorganisms and pathogens. Although the outermost layers—the stratum corneum and epidermis—consist of both living and dead cells, approximately 30,000 cells are shed from the surface every minute. These cells are continuously replenished by living cells generated in deeper layers of the epidermis. Beneath the epidermis lies the dermis, which contains blood vessels, nerve endings, and glands, while a subcutaneous fat layer provides insulation, cushioning, and an energy reserve.<sup>1</sup>

The shortage of donor tissue for skin grafting and the need for rapid skin regeneration have long been major challenges, particularly in extensive burns where autologous grafts are not available. Tissue-engineered skin substitutes have emerged as superior alternatives to conventional methods in treating full-thickness burns and traumatic injuries such as accidents or electrocution.<sup>2</sup>

The primary functions of wound dressings are to protect the wound from microbial contamination, support hemostasis, accelerate healing through exudate absorption and autolytic debridement, insulate the wound from temperature fluctuations, and maintain moisture balance between the wound and the dressing.<sup>3</sup> Throughout history, humans have sought effective remedies for wound healing, employing diverse natural and synthetic materials.<sup>4</sup> Ancient Egyptians, for example, used animal fats, honey, and plant fibers, while others experimented with tree bark, herbs, fabrics, and synthetic compounds—some effective, others ineffective or even toxic.

Contrary to the traditional belief that wounds heal faster when kept dry, Winter (1962) demonstrated that moist wound environments significantly accelerate healing compared to exposure to air.<sup>5,6</sup>

Subsequent studies confirmed this principle, which is now considered

fundamental in wound care. Mechanisms underlying moist wound healing include enhanced cell migration, stimulation of fibroblasts for collagen secretion, formation of a supportive matrix for enzyme and growth factor activity, macrophage activation, and facilitation of autolytic debridement.<sup>7</sup>

Tissue engineering and regenerative medicine, integrating evolutionary biology, life sciences, and engineering, aim to address clinical challenges by developing biological substitutes to restore, maintain, or improve tissue function. Since its formal definition in 1988, tissue engineering has increasingly focused on antimicrobial polymeric structures. Such polymers can be designed with intrinsic antimicrobial properties, modified to acquire these characteristics, or combined with organic and inorganic antimicrobial agents.<sup>8,9</sup>

Polyurethanes are particularly attractive due to their biocompatibility, mechanical strength, and versatility. By selecting appropriate components (polyols, diisocyanates, etc.), polyurethane can be tailored to specific applications and fabricated in various forms such as films, hydrogels, hydrocolloids, and foams. These structures can be engineered to achieve desired levels of water vapor permeability, mechanical durability, and biocompatibility. Moreover, antimicrobial agents such as quaternary ammonium salts and metallic ions (e.g., silver) have been successfully incorporated into polyurethane matrices. In this project, polyurethane films containing walnut leaf extract at different concentrations were developed as wound dressings.

An ideal skin substitute or dressing in tissue engineering should control fluid loss, maintain wound moisture, prevent infection, and minimize contraction and scarring.<sup>13</sup> To achieve this, the membrane must exhibit a gradient of pore sizes: approximately 150  $\mu\text{m}$  at the wound interface to facilitate fibroblast and keratinocyte infiltration, and 20–50  $\mu\text{m}$  at the outer surface to prevent

contamination and control fluid evaporation.<sup>14</sup>

Accordingly, the aim of this study was to fabricate and evaluate polyurethane films incorporated with walnut leaf extract for surgical wound healing, with the goal of achieving optimal porosity, moisture retention, bacterial resistance, and enhanced tissue regeneration.

## Materials and Methods

Polyurethane films were prepared by first dissolving polyurethane at a concentration of 12% in a mixed solvent system of tetrahydrofuran (THF) and dimethylformamide (DMF) in a 50:50 ratio. The solution was stirred magnetically for 3 h at 25°C to ensure complete dissolution and homogeneity. Subsequently, walnut extract was incorporated into the polyurethane solution at concentrations of 1, 2, and 4 wt%, and the resulting mixtures were stirred for an additional 1 h. In the final step, the prepared solutions were cast onto Teflon plates and dried in an oven at 40°C for 12 h to obtain the films.

## Morphological Analysis

To examine the morphology and internal structure of the films, the dried samples were cut into 1×11 × 11×1 cm pieces and coated with gold-palladium using a sputter coater to enhance surface conductivity and improve image quality. The surface and cross-sectional morphologies of the films were then observed using a scanning electron microscope (SEM, AIS2100C, Korea).

## Fourier Transform Infrared Spectroscopy (ATR-FTIR)

The functional groups and chemical bonds present in the films were identified using attenuated total reflectance Fourier transform infrared spectroscopy (ATR-FTIR) with an FTIR Ultrashield 400 MHz spectrometer (Bruker, Germany). Spectra were recorded in the range of 400–3500 cm<sup>-1</sup> at a resolution of 2 cm<sup>-1</sup>.

## Film Thickness Measurement

Film thickness was measured using a Mitutoyo micrometer with a resolution of 0.001 mm. Thickness was recorded at five randomly selected positions on each film, and the mean value was used for analysis.

## Turbidity and UV-Vis Analysis

The absorption and transmission spectra of the films were measured using a UV-Vis spectrophotometer (JASCO V-670, Japan) over the wavelength range of 190–900 nm, using air as the reference. The optical transparency of the films was calculated using Equation (1-3):

$$\text{Transparency} = -\log T_{600}/x \quad (1-3)$$

where T<sub>600</sub> is the transmittance at 600 nm and x is the film thickness.

## Mechanical Property Analysis

The mechanical properties of the prepared films were evaluated in accordance with the ASTM D882-10 standard using a universal testing machine (Instron 5566, USA). Rectangular film specimens, measuring 100 mm in length and 20 mm in width, were prepared and securely mounted between the tensile grips. The tests were conducted at a crosshead speed of 5 mm/min until sample rupture. All measurements were performed in triplicate, and the results are presented as mean values accompanied by their respective standard deviations.

## Water Contact Angle Analysis

To assess the surface hydrophilicity of the films, water contact angle measurements were performed using a goniometer (VCA Optima, AST Inc., USA). Square film samples (12 mm × 12 mm) were affixed to a horizontal support. A microsyringe was employed to deposit a 2 μL droplet of distilled water perpendicularly onto the film surface. To ensure statistical reliability, measurements were taken at five distinct locations on each sample. The droplet profile was captured 30 seconds post-deposition, and the contact angle was determined using the instrument's image analysis software.

## Water Absorption Capacity

The water absorption capacity of the films was determined following a modified ASTM-D-5964 standard, adapted for hydrogel-type materials. Square samples ( $1 \times 1 \text{ cm}^2$ ) were precisely weighed in their dry state. Subsequently, these samples were immersed in deionized water maintained at  $37^\circ$  for 24 hours. The water absorption percentage was calculated using Equation (2-3):

$$\text{Swelling ratio} = \left[ \frac{w_w - w_d}{w_d} \right] \times 100\% \quad (2-3)$$

where  $W_w$  represents the weight of the sample in the swollen (wet) state, and  $W_d$  is the initial dry weight of the sample. Post-incubation, the samples were carefully removed and blotted with filter paper for 5 minutes to eliminate surface moisture before determining their wet weight.

## Cytotoxicity Assay

Cytotoxicity was evaluated in accordance with ISO 10993-5. The film samples were sterilized via immersion in 70% ethanol and subsequently incubated in DMEM (Dulbecco's Modified Eagle Medium) to prepare sample extracts. Murine fibroblast L929 cells, sourced from the Encyto Pasteur Cell Bank (Tehran, Iran), were utilized and maintained as adherent cultures. Cells were seeded into 24-well plates at an initial density of 5,000 cells per well. Following seeding, the cells were exposed to culture medium supplemented with the prepared sample extracts. Cell viability was assessed at time points of 0, 24, 72, and 96 hours using the MTT assay. At each designated time point, the culture medium was removed, and the cells were washed with phosphate-buffered saline (PBS). Subsequently, 400  $\mu\text{L}$  of fresh culture medium and 40  $\mu\text{L}$  of MTT solution (5 mg/mL stock) were added to each well.

The plates were incubated at  $37^\circ\text{C}$  for 4 hours. Following incubation, the medium was carefully decanted, and 200  $\mu\text{L}$  of dimethyl sulfoxide (DMSO) was added to each well to dissolve the resulting formazan

crystals. Absorbance was subsequently measured at a wavelength of 540 nm.

## Evaluation of Cell Adhesion

To evaluate cell adhesion and morphology on films containing ethanolic propolis extract and hyaluronic acid, the samples were incubated for 5 days. After the incubation period, the culture medium was removed, and the adhered cells were fixed using a 4% glutaraldehyde solution for 30 minutes. The samples were then dehydrated through a graded ethanol series (50%, 70%, 90%, and 100%), followed by storage in absolute ethanol prior to observation via scanning electron microscopy (SEM).

## Statistical Analysis

All data are presented as mean  $\pm$  standard deviation (mean  $\pm$  SD). Statistical analysis was conducted using SPSS software (version 16.0). One-way analysis of variance (ANOVA) was employed to compare differences between groups, with statistical significance defined as  $P < 0.05$ .

## Findings

### Morphological Observation and Microstructural Analysis

To investigate the surface topography of the films, scanning electron microscopy (SEM) was employed. As shown in Figure 1, the neat polyurethane (PU) film exhibited a smooth and uniform microstructure without any cracks, pores, or defects. In contrast, the surface of PU films containing 1%, 2%, and 4% walnut leaf extract displayed a rough and three-dimensional morphology. The hill-like protrusions observed on the film surface correspond to the presence and distribution of walnut leaf extract within the polymer matrix. This increase in surface roughness can be attributed to the oxidation of phenolic compounds in the extract into quinones, which subsequently aggregate and form relatively large domains within the polymer network. Previous studies have demonstrated that surfaces with greater roughness provide a more favorable

environment for cell adhesion and proliferation.<sup>15,16</sup>

### ATR-FTIR Analysis

This test was conducted to verify the chemical composition of the wound dressing, specifically the incorporation of walnut leaf extract into the polyurethane matrix. Figure 2 presents the FTIR spectrum of walnut leaf extract, while Figure 3 shows the spectrum of polyurethane and the polyurethane–walnut extract composite film.

In Figure 2, the functional groups of the walnut leaf extract are clearly identified. The absorption band at  $3200\text{ cm}^{-1}$  corresponds to the stretching vibration of phenolic O–H groups. The resonance of aromatic C=C bonds is observed at  $1603\text{ cm}^{-1}$ . Aliphatic C–H stretching vibrations appear in the region of  $2850\text{--}3000\text{ cm}^{-1}$ . The bands between  $1030\text{--}1200\text{ cm}^{-1}$  indicate C–O stretching and secondary alcohol O–H vibrations.<sup>16</sup>

**Polyurethane FTIR Spectrum** In the polyurethane spectrum, the  $\text{CH}_2$  stretching vibration is observed at  $2931\text{ cm}^{-1}$ , while the N–H bending vibration appears at  $1557\text{ cm}^{-1}$ . The C–N stretching band is detected at  $1063\text{ cm}^{-1}$ . A broad absorption band between  $3200\text{--}3500\text{ cm}^{-1}$  corresponds to N–H stretching, and a distinct peak at  $1732\text{ cm}^{-1}$  confirms the presence of carbonyl (C=O) groups in the polyurethane structure.<sup>17</sup>

In the FTIR spectrum of the polyurethane–walnut extract composite film, the characteristic peaks of both walnut leaf extract and polyurethane are present,

indicating the coexistence of the two components without the formation of new chemical bonds.

### Mechanical Properties Evaluation

Mechanical strength is a critical property for wound dressings, as they must be durable and resistant to external stresses while maintaining elasticity, particularly in highly mobile regions such as the knee and elbow.<sup>18</sup>

Table 1 illustrates the effect of incorporating different concentrations of walnut leaf extract on the tensile strength (TS) and elongation at break (SB) of polyurethane films. As observed, the addition of walnut leaf extract from 0% to 1% reduced the ultimate tensile strength (UTS) from  $6.62 \pm 1.2\text{ MPa}$  to  $6.34 \pm 0.5\text{ MPa}$ , while elongation at break increased from  $38.4 \pm 4.7\%$  to  $42.91 \pm 1.2\%$ . The presence of the extract disrupts the continuity of the polyurethane network, thereby decreasing mechanical strength but enhancing flexibility. Since walnut leaf extract lacks a polymeric structure, its incorporation weakens the polymer matrix and introduces discontinuities. At higher concentrations (2% and 4%), tensile strength further decreased to  $6.08 \pm 1.5\text{ MPa}$  and  $4.47 \pm 0.9\text{ MPa}$ , respectively, while elongation at break increased to  $44.71 \pm 9.6\%$  and  $68.24 \pm 11\%$ . These results confirm that walnut leaf extract progressively reduces the Young's modulus of the films, making them more flexible but less mechanically robust.

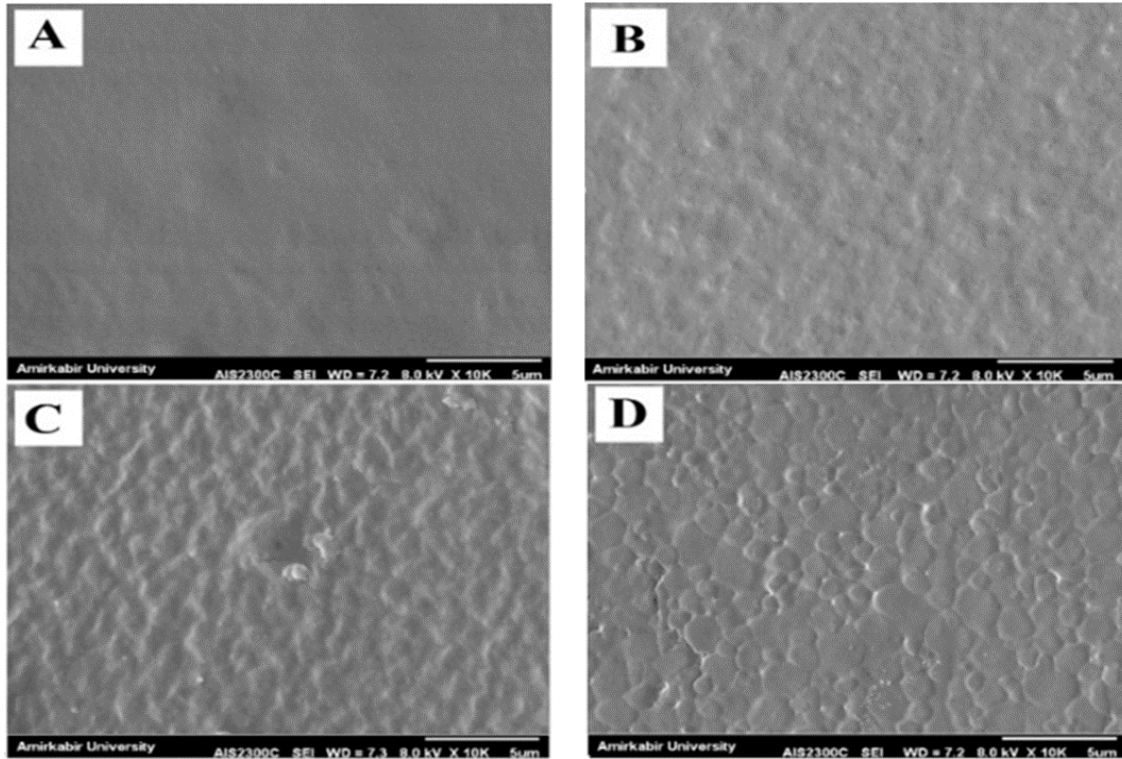


**Figure 1-** SEM micrographs of the film-based wound dressings: (A) neat PU, (B) PU containing 1% extract, (C) PU containing 2% extract, and (D) PU containing 4% extract

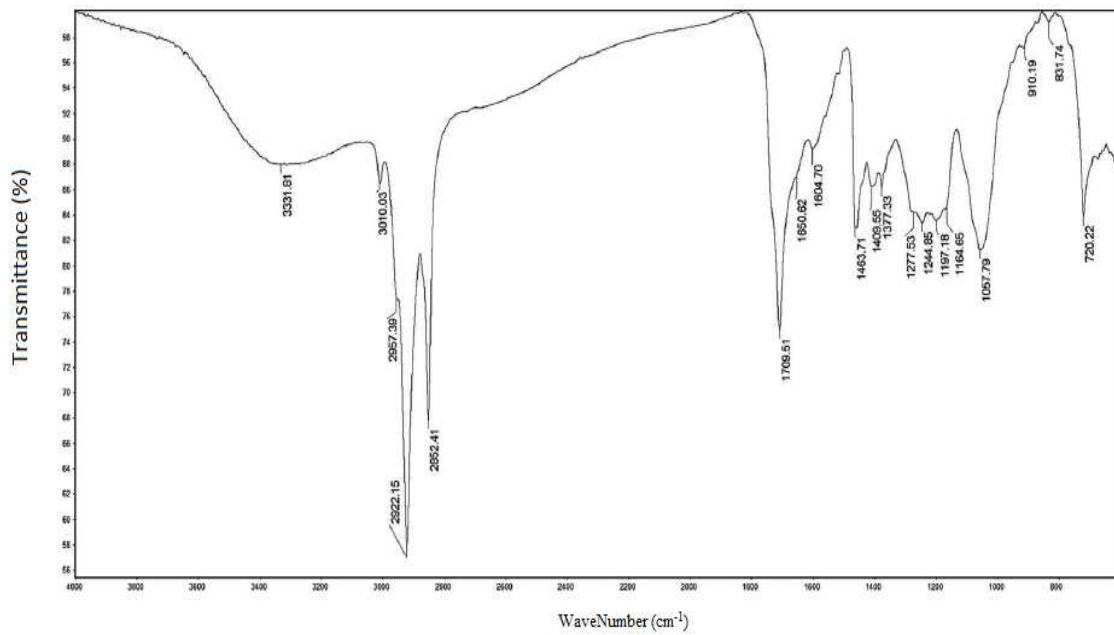


**Figure 2-** FTIR spectrum of walnut leaf extract

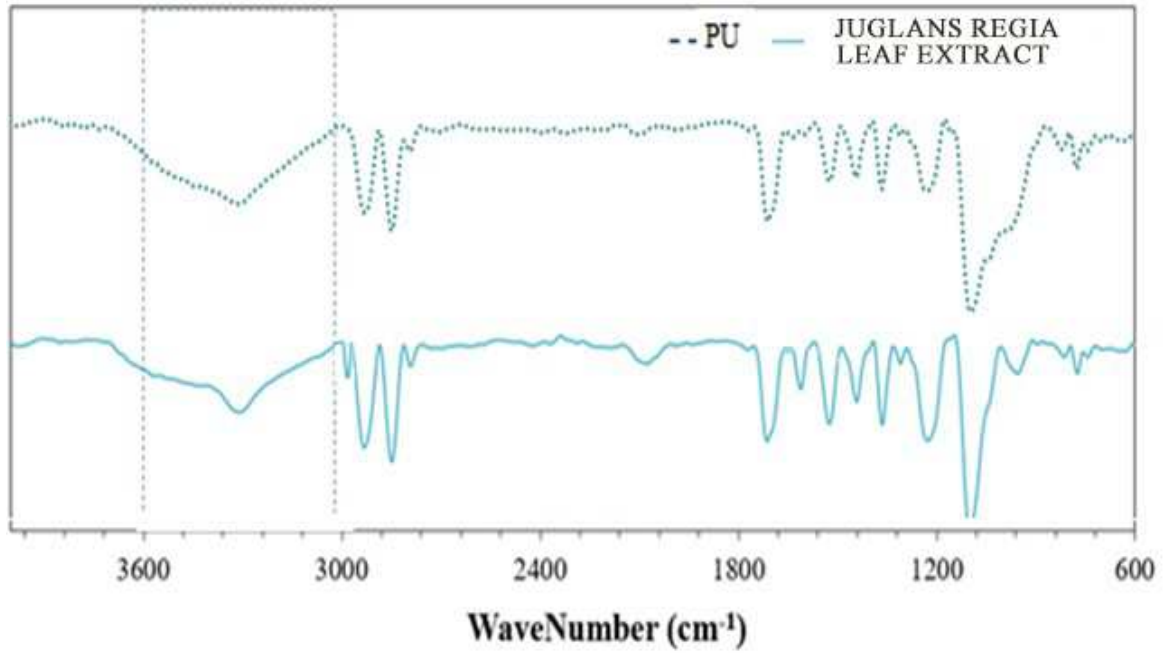


Figure 3- FTIR spectra of polyurethane (PU) and polyurethane-walnut leaf extract composite films

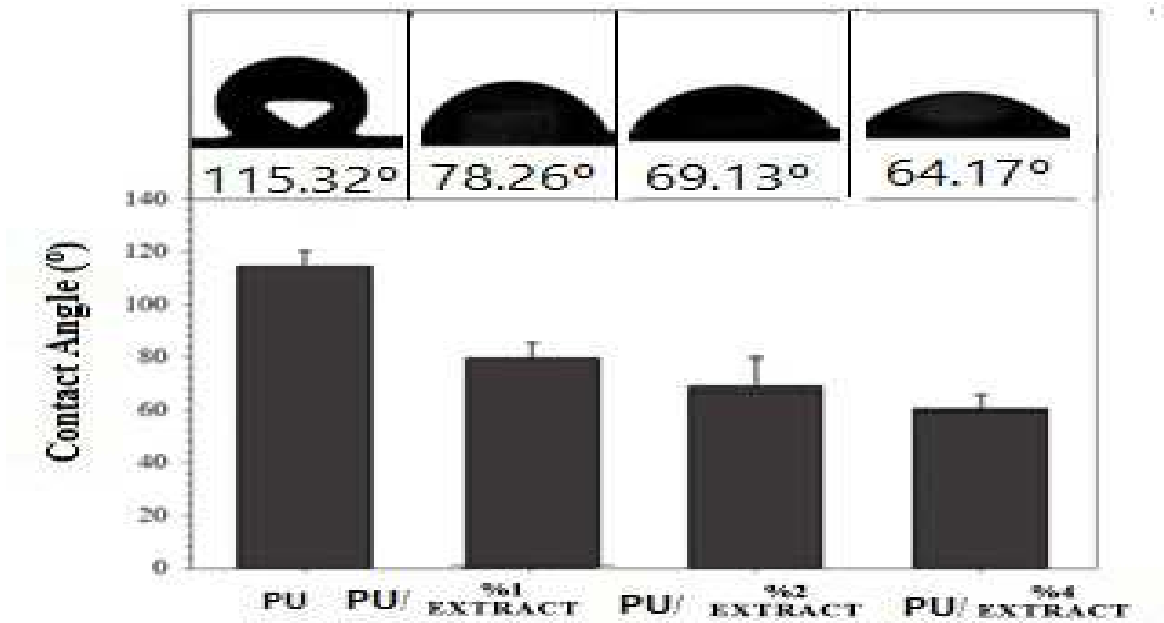
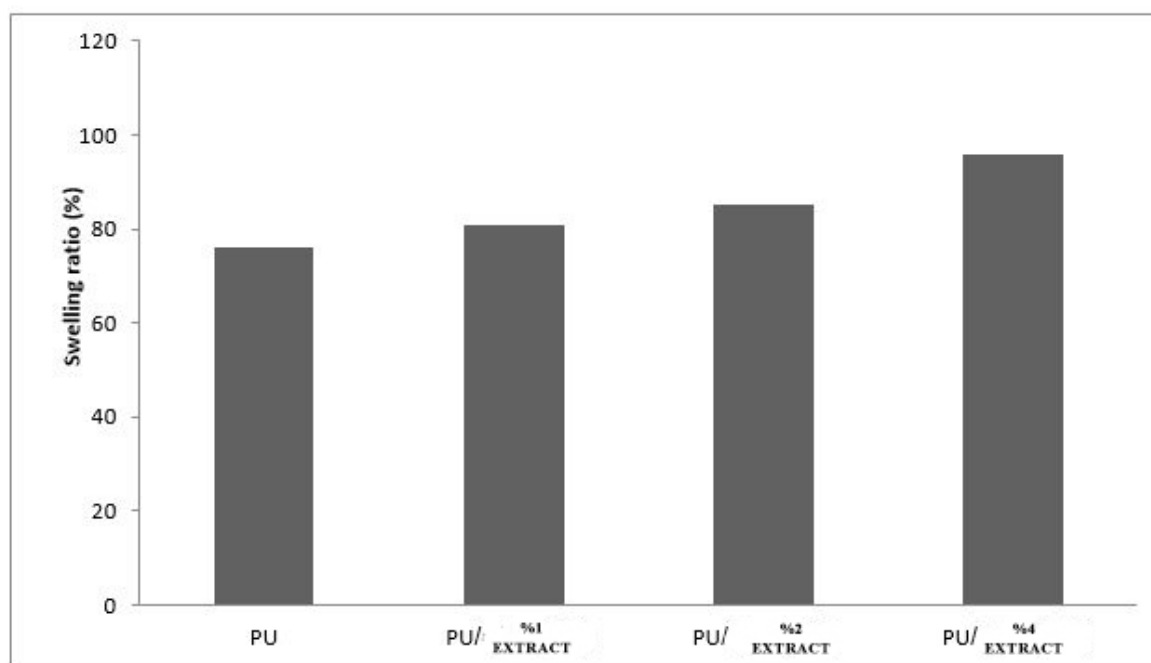


Figure 4- Water contact angle images of the film surfaces in the contact-angle measurement test

**Table 1- Mechanical properties test**

<i>Sample</i>	<i>Tensile strength (MPa)</i>	<i>Young's modulus (MPa)</i>	<i>Strain at break (%)</i>	<i>Thickness (mm)</i>
<i>PU</i>	$6/62 \pm 1/2$	$15/4 \pm 5/2$	$38/4 \pm 4/7$	$0/125 \pm 0/017$
<i>PU/ Extract(%1)</i>	$6/34 \pm 0/5$	$14/9 \pm 5/7$	$42/91 \pm 1/2$	$0/120 \pm 0/039$
<i>PU/ Extract(%2)</i>	$6/08 \pm 1/5$	$13/5 \pm 3/2$	$44/71 \pm 9/6$	$0/117 \pm 0/008$
<i>PU/ Extract(%4)</i>	$4/47 \pm 0/9$	$9/6 \pm 3/5$	$68/24 \pm 11/3$	$0/121 \pm 0/022$

**Figure 5- PBS Absorption Profile of PU, 1% Extract/PU, 2% Extract/PU, and 4% Extract/PU Samples After 24 Hours**

## Contact Angle Analysis

Contact angle measurement is a reliable technique for evaluating the wettability of polymeric surfaces. Hydrophilic surfaces are essential for wound dressings and tissue-engineering scaffolds, as increased wettability enhances biocompatibility and dressing performance.<sup>18</sup> In this study, contact angle analysis was performed for four samples: PU, 1% extract/PU, 2% extract/PU, and 4% extract/PU. As shown in Figure 4, the neat PU film exhibited a contact angle of 115.032°. In contrast, the films containing 1%, 2%, and 4% walnut leaf extract showed contact angles of 78.026°, 69.013°, and 64.017°, respectively. The incorporation of walnut leaf extract significantly reduced the contact angle due to the presence of hydrophilic O–H functional groups, thereby increasing the hydrophilicity of the composite films.

## Swelling and Exudate Absorption

The accumulation of wound exudate can promote bacterial colonization and impede the healing process; therefore, a high exudate absorption capacity is a crucial characteristic of an effective wound dressing.<sup>19</sup> In this study, the swelling capacity of the films was quantified by measuring the percentage of PBS absorption following 24 hours of immersion.

As depicted in Figure 5, the neat polyurethane (PU) film demonstrated 76% PBS absorption. The incorporation of walnut leaf extract resulted in a concentration-dependent increase in absorption, reaching 81%, 85%, and 96% for the 1%, 2%, and 4% extract/PU samples, respectively. This observed enhancement in swelling is attributed to the presence of hydrophilic functional groups within the walnut leaf extract, which elevate the affinity of the polymeric matrix for aqueous media.

## In Vitro Degradation Study

The degradation rate of wound dressings is significantly influenced by the polymer's inherent hydrophilicity and the flexibility of its polymer chains. Highly crystalline polymers typically exhibit more rigid chain

structures, which tend to impede microbial or enzymatic access to reactive sites, consequently prolonging the degradation period. In this investigation, 41% of the neat polyurethane (PU) film's initial mass remained after eight weeks of degradation. Conversely, the incorporation of walnut leaf extract demonstrably accelerated the degradation process. Specifically, 32%, 25%, and 21% of the initial mass remained for the 1%, 2%, and 4% extract/PU samples, respectively. These findings suggest that the enhanced hydrophilicity and increased chain flexibility conferred by the walnut extract facilitated more rapid hydrolytic degradation, as further illustrated in Figure 6.

## UV-Vis Transmission and Transparency

The light transmission properties of the developed films were thoroughly investigated to ascertain their efficacy in blocking ultraviolet (UV) radiation. The experimental results clearly indicate that the incorporation of walnut leaf extract into the polyurethane matrix significantly enhances UV absorption.<sup>20</sup> This effect is primarily attributed to the presence of phenolic compounds and flavonoids within the extract, which are molecular structures characterized by unsaturated double bonds capable of effectively absorbing UV radiation. These observations align with existing literature. For example, Gómez et al. previously demonstrated that the integration of various natural extracts, including rosemary, marjoram, and oregano, into biopolymer films markedly improves their UV-blocking capabilities.<sup>21,22</sup> Their research specifically noted that the presence of polyphenols in gelatin-based films resulted in a reduction in light transmission and a concurrent increase in UV absorption within the 200–350 nm wavelength range.<sup>23</sup> Therefore, the results obtained in this study (as presented in Figure 7) corroborate that the inclusion of walnut leaf extract within the PU matrix effectively enhances the film's UV-shielding performance.

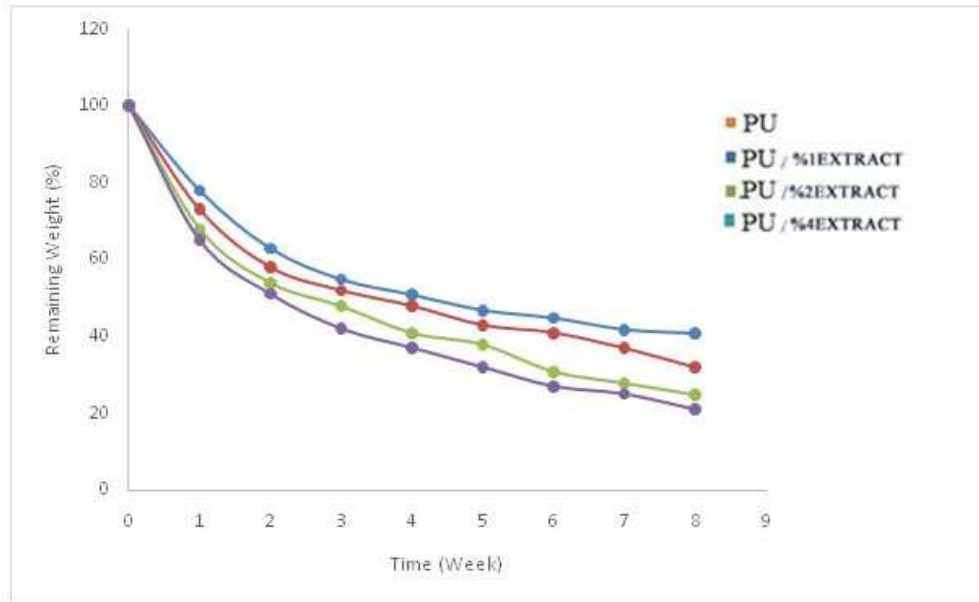


**Figure 6- Degradation study of PU, (1%) extract/PU, (2%) extract/PU and (4%) extract/PU samples over 8 weeks**

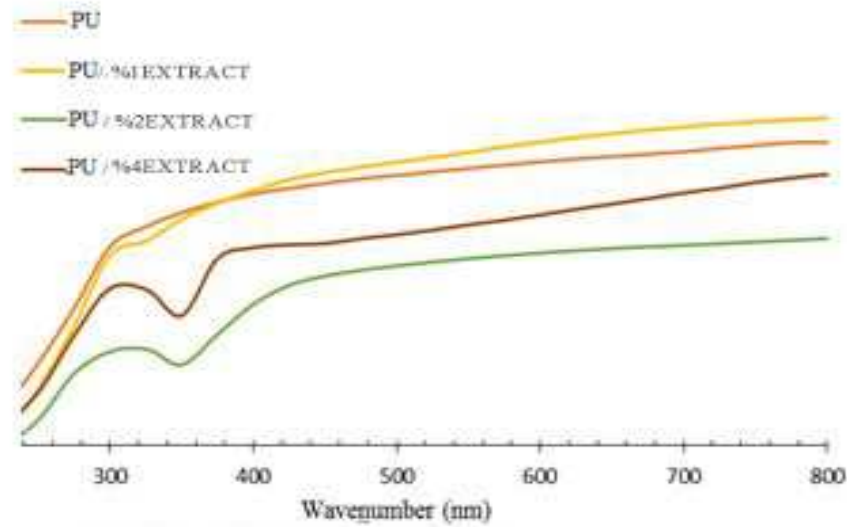


**Figure 7- UV-Vis Spectra of PU, 1% Extract/PU, 2% Extract/PU, and 4% Extract/PU Samples**

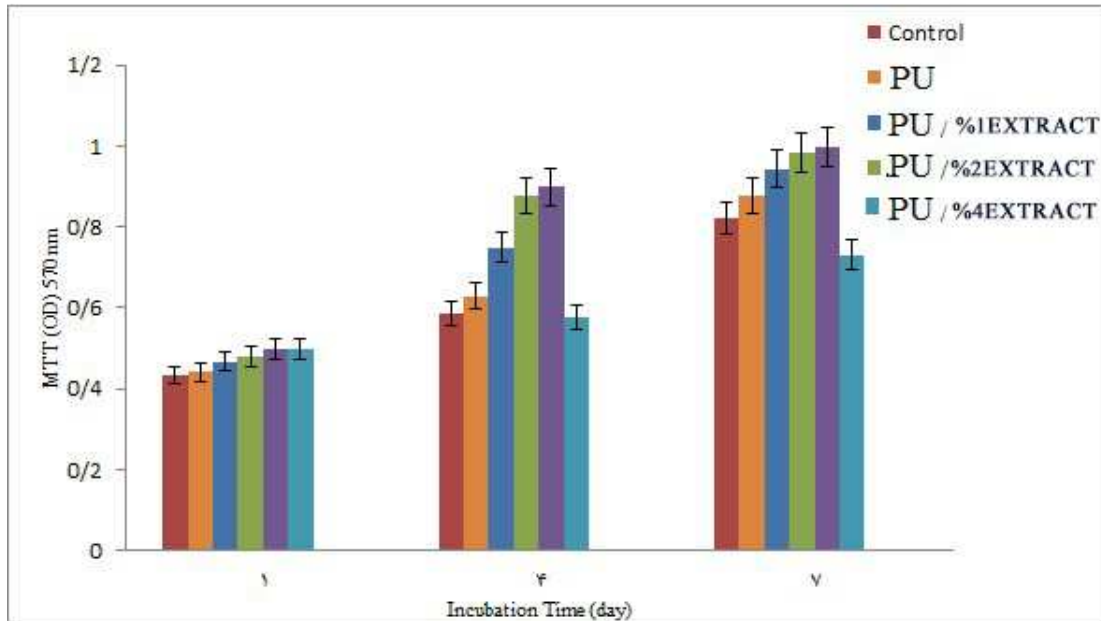


**Figure 8-** Graph of MTT assay results showing cell growth on the films after 1, 4, and 7 days of culture, with statistically significant differences ( $P < 0.05$ ).

### Fibroblast Proliferation and Viability

Cell proliferation on the prepared films was evaluated using the MTT assay. To assess cytotoxicity, L929 fibroblast cells were cultured in the presence of PU, 1% extract/PU, 2% extract/PU, and 4% extract/PU films for seven days. As shown in Figure 8, the 4% extract/PU film (containing 4% walnut leaf extract) exhibited noticeable cytotoxicity on day 7 compared to films with lower extract concentrations (1% and 2% extract/PU), with statistically significant differences ( $P < 0.05$ ). This reduction in cell growth may be attributed to the release of potentially harmful compounds, such as caffeic acid derivatives. In contrast, the highest cell viability was observed in the 2% extract/PU film ( $P < 0.05$ ). These findings

highlight the beneficial effects of walnut leaf extract at concentrations of 1% and 2%, which enhance substrate hydration, promote fibroblast aggregation, and reduce cytotoxicity. Overall, the MTT assay results demonstrated increased fibroblast growth and proliferation in films containing low-to-moderate levels of walnut leaf extract.

After seven days of cell culture, optical microscopy images of the films were examined (Figure 9). These images clearly demonstrate that fibroblast cells on PU, 1% extract/PU, and 2% extract/PU films exhibited superior growth compared to the control and the 4% extract/PU film. Ultimately, the films containing 2% walnut leaf extract supported the highest level of fibroblast proliferation, providing a favorable substrate for cell attachment and growth.

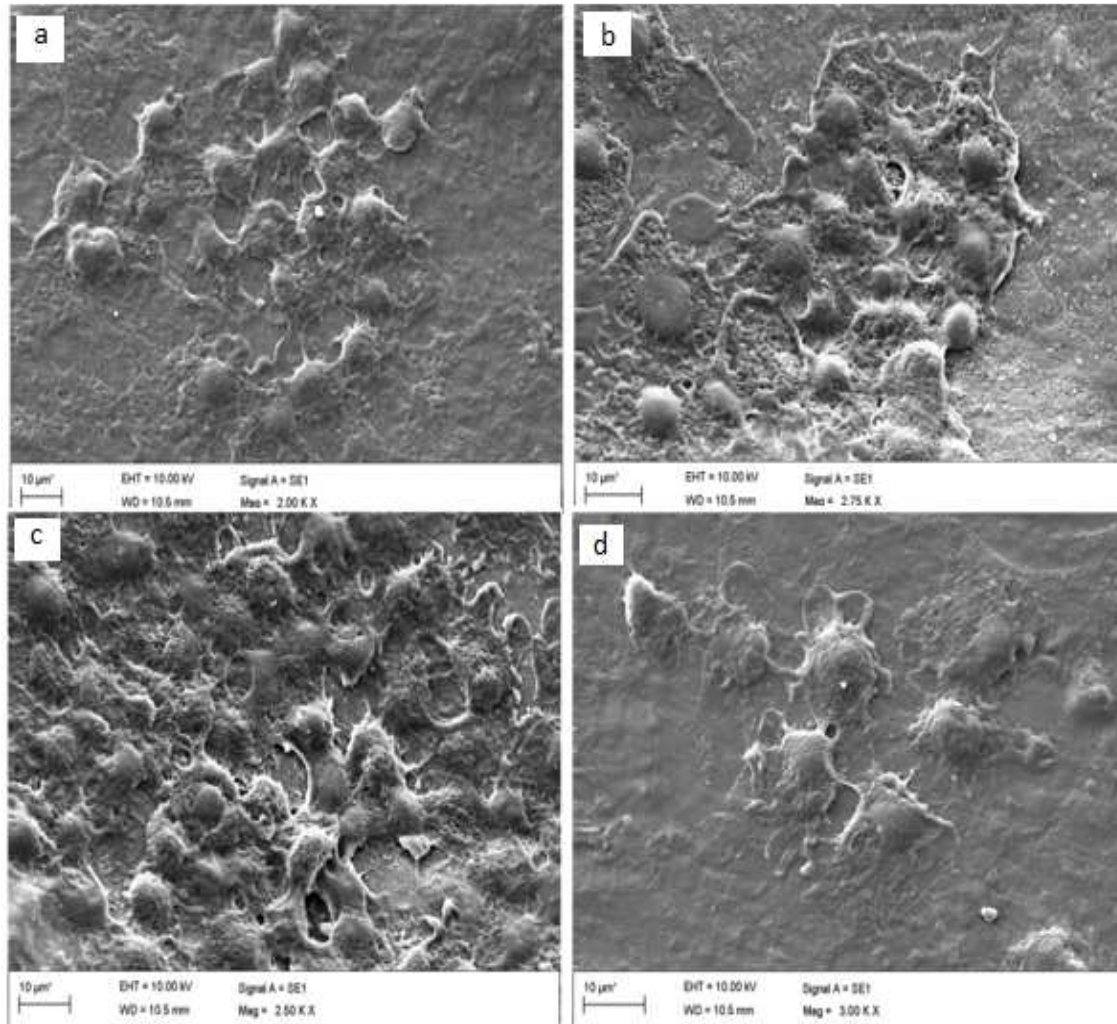


**Figure 9- SEM images of fibroblast growth on film-based wound dressings: A) PU, B) 1% extract/PU, C) 2% extract/PU, and D) 4% extract/PU after seven days of culture**

## Discussion and Conclusion

Overall, the findings of this study can be summarized as follows:

1. Polyurethane–extract films were successfully fabricated using the casting method.
2. Uniform films were obtained by incorporating polyurethane with walnut leaf extract at concentrations of 1%, 2%, and 4% (w/w).
3. The tensile strength of pure polyurethane films was  $6.62 \pm 1.2$  MPa,

which decreased to  $4.47 \pm 0.9$  MPa upon the addition of walnut leaf extract.

4. Incorporation of 4% (w/w) walnut leaf extract increased elongation at break, indicating enhanced flexibility.

5. Film transparency and light transmittance decreased with increasing extract content.

6. In degradation tests, 41% of the pure polyurethane film remained intact after eight weeks. With the addition of walnut leaf extract, the residual mass decreased to 32%, 25%, and 21% for 1%, 2%, and 4% extract/PU films, respectively.

7. MTT assay results revealed that the highest cell viability was observed in films containing 2% extract/PU. In contrast, the 4% extract/PU film exhibited noticeable cytotoxicity on day 7 compared to films with lower extract concentrations ( $P < 0.05$ ).

8. SEM analysis demonstrated that fibroblast cells adhered and proliferated

more effectively on PU, 1% extract/PU, and 2% extract/PU films compared to the control and the 4% extract/PU film.

9. In this study, films containing 2% walnut leaf extract provided the most favorable substrate for fibroblast growth, supporting enhanced cell adhesion and proliferation.

## References:

1. F. Groeber, M. Holeiter, M. Hampel, S. Hinderer, and K. Schenke-Layland, "Skin tissue engineering-in vivo and in vitro applications," *Advanced drug delivery reviews*, vol. 63, pp. 352-366, 2011.
2. Y.-F. Goh, I. Shakir, and R. Hussain, "Electrospun fibers for tissue engineering, drug delivery, and wound dressing," *Journal of Materials Science*, vol. 48, pp. 3027-3054, 2013.
3. S. Kishida, "Nanoscale biological and physical factors influence on myogenic differentiation of skeletal myoblasts," 2014.
4. B. Chevally and D. Herbage, "Collagen-based biomaterials as 3D scaffold for cell cultures: applications for tissue engineering and gene therapy," *Medical and Biological Engineering and Computing*, vol. 38, pp. 211-218, 2000.
5. J. A. Sherratt and J. C. Dallon, "Theoretical models of wound healing: past successes and future challenges," *Comptes Rendus Biologies*, vol. 325, pp. 557-564, 2002.
6. R. White and K. F. Cutting, "Modern exudate management: a review of wound treatments," *World Wide Wounds*, vol. 2006, 1.
7. G. S. Lazarus, D. M. Cooper, D. R. Knighton, D. J. Margolis, R. E. Percoraro, G. Rodeheaver, et al., "Definitions and guidelines for assessment of wounds and evaluation of healing," *Wound Repair and Regeneration*, vol. 2, pp. 165-170, 1994.
8. J. Hilton, D. Williams, B. Beuker, D. Miller, and K. Harding, "Wound dressings in diabetic foot disease," *Clinical Infectious Diseases*, vol. 39, pp. S100-S103, 2004.
9. M. C. Ferreira, P. Tuma Júnior, V. F. Carvalho, and F. Kamamoto, "Complex wounds", *Clinics*, vol. 61, pp. 571-578, 2006.
10. L. S. Nair and C. T. Laurencin, "Biodegradable polymers as biomaterials," *Progress in polymer science*, vol. 32, pp. 762-798, 2007.
11. J.-P. Chen, G.-Y. Chang, and J.-K. Chen, "Electrospun collagen/chitosan nanofibrous membrane as wound dressing," *Colloids and Surfaces A: Physicochemical and Engineering Aspects*, vol. 313, pp. 183-188, 2008.
12. G. D. Mogoşanu and A. M. Grumezescu, "Natural and synthetic polymers for wounds and burns dressing," *International journal of pharmaceuticals*, vol. 463, pp. 127-136, 2014.
13. R. A. Kamel, J. F. Ong, E. Eriksson, J. P. Junker, and E. J. Caterson, "Tissue engineering of skin," *Journal of the American College of Surgeons*, vol. 217, pp. 533-555, 2013.
14. T. W. Wang, H. C. Wu, Y. C. Huang, J. S. Sun, and F. H. Lin, "Biomimetic Bilayered Gelatin-Chondroitin 6 Sulfate-Hyaluronic Acid Biopolymer as a Scaffold for Skin Equivalent Tissue Engineering," *Artificial organs*, vol. 30, pp. 141-149, 2006.
15. A. D. Association, "Diagnosis and classification of diabetes mellitus," *Diabetes care*, vol. 37, pp. S81-S90, 2014.
16. A. A. Chaudhari, K. Vig, D. R. Baganizi, R. Sahu, S. Dixit, V. Dennis, et al., "Future prospects for scaffolding methods and biomaterials in skin tissue engineering: a review," *International journal of molecular sciences*, vol. 17, p. 1974, 2016.
17. S. G. Priya, H. Jungvid, and A. Kumar, "Skin tissue engineering for tissue repair and regeneration," *Tissue Engineering Part B: Reviews*, vol. 14, pp. 105-118, 2008.
18. L. I. Moura, A. M. Dias, E. Carvalho, and H. C. de Sousa, "Recent advances on the development of wound dressings for diabetic foot ulcer treatment-a review," *Acta biomaterialia*, vol. 9, pp. 7093-7114, 2013.
19. R. A. Clark, K. Ghosh, and M. G. Tonnesen, "Tissue engineering for cutaneous wounds," *Journal of Investigative Dermatology*, vol. 127, pp. 1018-1029, 2007.
20. K. M. Woo, V. J. Chen, and P. X. Ma, "Nano-fibrous scaffolding architecture selectively enhances protein adsorption contributing to cell attachment," *Journal of biomedical materials research Part A*, vol. 67, pp. 531-537, 2003.
21. F. J. O'Brien, "Biomaterials & scaffolds for tissue engineering," *Materials today*, vol. 14, pp. 88-95, 2011.
22. B. Dhandayuthapani, Y. Yoshida, T. Maekawa, and D. S. Kumar, "Polymeric scaffolds in tissue engineering application: a review," *International Journal of Polymer Science*, vol. 2011, 2011.
23. J. Santerre, K. Woodhouse, G. Laroche, and R. Labow, "Understanding the biodegradation of polyurethanes: from classical implants to tissue engineering materials," *Biomaterials*, vol. 26, pp. 7457-7470, 2005.
24. M. C. Ferreira, P. Tuma, Jr., V. F. Carvalho, and F. Kamamoto, "Complex wounds," *Clinics (Sao Paulo)*, vol. 61, pp. 571-8, Dec 2006.
25. G. Broughton 2<sup>nd</sup>, J. E. Janis, and C. E. Attinger, "The basic science of wound healing," *Plastic and reconstructive surgery*, vol. 117, pp. 12S-34S, 2006.
26. J. Schilling, "Wound care made incredibly visual. USA: Lippincott Williams & Wilkins," 2007.